

EXPLORING HUMAN BRAIN ACTIVATION VIA NESTED SPARSE CODING AND FUNCTIONAL OPERATORS

Shu Zhang¹, Xiang Li¹, Lei Guo², Tianming Liu¹

¹Cortical Architecture Imaging and Discovery Lab, Department of Computer Science and Bioimaging Research Center, The University of Georgia, GA, USA; ²School of Automation, Northwestern Polytechnical University, Xi'an, China

ABSTRACT

Traditional task-based fMRI activation detection methods, such as the general linear model (GLM), assume that the fMRI signals of activated brain regions follow the external stimulus paradigm. Typically, these activated regions are detected independently in a voxel-wise fashion, and the interaction among voxels is nevertheless neglected. Despite the wide use and remarkable success of GLM, the temporal and spatial relationships among activated regions remain unveiled. In response to this challenge, we present a novel method that combines two-stage sparse representation framework and the operator modulations (integral and derivative) to explore the temporal and spatial organizations underlying fMRI-derived activations in the brain. The two-stage sparse representation framework is designed to deal with big data and the functional operator is focused on finding the refined activation areas in the brain under task performances. Experiments demonstrated that diverse temporal and spatial organizations between activated regions exist and different functional operators may lead to different activation areas, thus significantly supplementing to the available principle of GLM that has been widely used in the human brain mapping field.

Index Terms— Functional Operator, Activation Detection, Nested Sparse Codings.

1. INTRODUCTION

Voxel-based activation detection in task-based fMRI has been widely used in the human brain mapping field. For instance, the general linear model (GLM) [1, 2] has been commonly used to determine activated voxels in task-based fMRI images due to its effectiveness, simplicity, robustness and wide availability [1, 3]. However, the behavior of the functioning brain is largely at network level [4], involving multiple distinct brain regions which continuously interact with each other. For example, some small regions belonging to the activation areas may participate in several functional brain networks during the fMRI scan. Thus, it is not enough to represent the activation areas only by the single spatial pattern which is obtained by GLM. In order to provide a better understanding of the organizational mechanism of the

functional brain and inspired by the theory of proportional-integral-derivative (PID) controller [5] which has been used in many research studies (e.g. in [6]), in this work we have presented a novel concept of functional brain operators and its corresponding analysis framework, aiming at the further refinement of the traditional activation detection results. The proposed framework utilizes the operators of integral and derivative for the temporal characterizations of the brain networks, which are the fundamental functions in the signal processing field.

Inspired by the successes of using sparse representation in pattern recognition [7, 8] and in functional brain imaging analysis [9, 10], in this work, the nested dictionary learning method [11] has been chosen for the analysis of fMRI signals, which is a two-stage framework by coupling the dictionary learning results from individual datasets into a second-stage dictionary learning routine. It has been shown in our prior studies [11] that it could potentially deal with the common problems in fMRI signal processing including inter-subject variability [12], big data, and noise [13].

In brief, in this work, we will first apply the nested sparse coding representation framework on the given fMRI dataset. Then the functional operators will be applied to the nested dictionary learning results, aiming to identify brain regions that: 1) have been detected by the GLM-based activation detection method but actually belong to different modulation types (integral, derivative, or unmodulated); and 2) have not been detected by the GLM-based activation detection method but have revealed by the functional operator analysis.

2. METHODS

2.1. Overview

As shown in Fig. 1, input fMRI signals will be first analyzed by nested dictionary learning and sparse coding method to obtain its atomic basis functional components with specified temporal and spatial patterns (a). Then the second-order discrete integrals and derivatives of the component's temporal activation pattern are obtained, deriving the

components' modulated temporal activation patterns (b). At the same time, stimulus paradigm is convoluted with the hemodynamic function as the template to match with each modulation (c). Then the correspondence between second-stage modulated functional components and task stimulus is identified by the matched pairs based on Pearson's correlation value (d). Trace-back method is finally used to identify the first-stage functional components which have relationship with activation detection after applying operators (e).

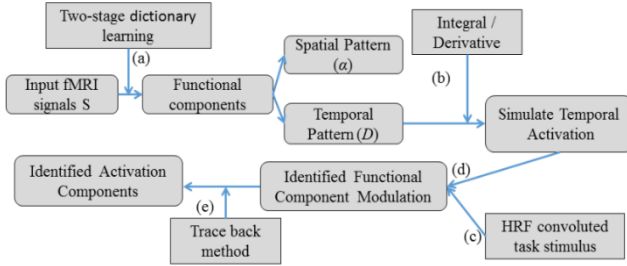


Fig.1. Overview of the proposed framework to identify activation components using the operators and nested sparse coding representation.

2.2. Data Acquisition and Pre-processing

The dataset used in this work comes from the Human Connectome Project (HCP) Q1 release [14]. The acquisition parameters of fMRI are: 90×104 matrix, 220mm FOV, 72 slices, $TR=0.72s$, $TE=33.1ms$, flip angle= 52° , $BW=2290$ Hz/Px, 2.0mm isotropic voxels. Preprocessing pipelines includes motion correction, spatial smoothing, temporal pre-whitening, slice time correction, and global drift removal. More detailed data acquisition and preprocessing are referred to [14]. In this work, fMRI data from seven tasks are used: working memory (WM) (405 volumes), gambling (253 volumes), language (316 volumes), emotion processing (176 volumes), motor (284 volumes), social cognition (274 volumes) and relational processing (232 frames).

2.3. Sparse representation of whole brain fMRI signals

2.3.1 First-stage sparse coding

In the first stage, the effective online dictionary learning algorithm [7] is chosen to learn a dictionary with sparsity constraint from the whole-brain fMRI signals of each subject. The time length is t and voxel numbers are represented by n . The algorithm would learn a meaningful and over-complete dictionary D [10, 11]. The dictionary is consisting of k atoms ($m > t$, $m \ll n$). The input matrix M is represented by dictionary D and corresponding sparse loading coefficient matrix α . In this way, each signal from M can be represented by the most relevant atoms in the dictionary D we learned. In previous studies, e.g., in [15], the assumption is well recognized that in fMRI data, each voxel's fMRI signal is a linear combination of several

atomic components. Thus, each signal from M will be represented by the most relevant atoms in the resultant dictionary D .

To be clearer, we use equations below to explain the basic steps. For the input fMRI signals, set $M = [m_1, m_2, \dots, m_n] \in \mathbb{R}^{t \times n}$ and the loss function for the dictionary learning algorithm to minimize is defined in Eq. (1) with a l_1 regularization that yields to a sparse constraint to the loading coefficient α (constrained by non-negativity), where λ is a regularization parameter to trade-off the regression residual and sparsity level:

$$\min_{D \in \mathbb{R}^{t \times k}, \alpha \in \mathbb{R}^{k \times n}} \frac{1}{2} \|M - D\alpha\|_F + \lambda \|\alpha\|_{1,1} \quad (1)$$

To prevent D to be arbitrarily large and lead to trivial solution of optimization, its columns are constrained by Eq. (2).

$$C \triangleq \{D \in \mathbb{R}^{t \times k} \text{ s.t. } \forall j = 1, \dots, k, d_j^T d_j \leq 1\} \quad (2)$$

To achieve the optimization, the procedure is done by iteratively updating D and α in Eq. (1). From the equations above, there are two important parameters we concerned. The value of λ and dictionary size k_1 , which are determined experimentally in literature studies ($\lambda=0.1$, $k_1=400$) [9, 10]. When the dictionary learning step is finished, the resulting D matrix contains temporal variations for each component, while the corresponding sparse loading coefficient matrix α contains the spatial distribution for each component.

2.3.2 Second-stage sparse coding method

Since we already have the first-stage dictionary learning results, our task is to obtain group-wise characterization of the dictionaries that could reveal the distinctive organization patterns among a group of subjects. So we need to build a new input for the second-stage dictionary learning. Thus, we combine all the subjects' D matrix into one big data matrix. We named it M^* , and then it will be used as the input for second-stage sparse-coding representation. In the second round, the parameters are $\lambda=0.1$, $k_2=50$, aiming to obtain a group-wise common dictionary D^* and the corresponding loading coefficients α^* , which could reflect the groupwise temporal and spatial organization patterns of the given dataset. Compared with the original fMRI data which are defined on the whole brain voxels, two-stage framework achieves a huge size reduction while still maintaining the major functional characterization for each individual [11]. More importantly, noises and undesired voxel-wise signal fluctuations are largely removed in M^* , thus we can ensure that most of the common dictionaries can represent the groupwise consistent functional activities, and their differences are more likely to be originated from the intrinsic features of functional brain activity patterns. Since first-stage components can be represented by linear combination of several functional components in the second stage, the most important reason that we need nested sparse

representation method is that we can track back the functional components in the first-stage to identify whether they have strong relationships or not.

2.4. Using Pearson correlation to identify functional components in the second stage

After obtaining the second-stage functional components, we use the commonly used Pearson's correlation to measure the temporal correlation between functional components and task design. Here, the temporal signals of the functional components need to be applied by operator functions (integral and derivative) and the signals of the task design need to be convoluted by Hemodynamic Response Function (HRF). Then the second stage component which has the highest correlation with convoluted task design will be picked up. That is, for each task, we will pick up two second-stage function components, one for each operator. Then the second-stage components will be used to identify functional components in the first-stage, and the details are shown in Section 2.5.

2.5. Trace-back method to identify function components in the first-stage

Based on the identified common functional components on the second-stage dictionary learning, the relationship between functional components is at individual subject level. In order to check the components in subject's level, we need to apply the D and α from the first-stage dictionary learning. As we know, for each component in the second stage, it corresponds to a vector in α , and this vector has 400 values with correspondences to 400 components. In most cases the value equals to 0, because this is a sparse matrix, where 0 represents that this signal will not be represented by the correspondence component. When the value becomes larger, the relationship will become close. In this paper, we experimentally set up a threshold ($T=0.2$) to pick up the dictionary atoms which has high relationship with the functional component we identified from the second-stage. After we pick up the dictionary atoms from the first-stage dictionary learning, we can obtain the spatial map and other details from the exact component. Here we emphasize that with the help from the groupwise second-stage functional components, the track-back method can help us identify the first-stage functional components that have strong correlation. Though these components may have almost different temporal signals, their signals may consist of several basic second-stage functional components.

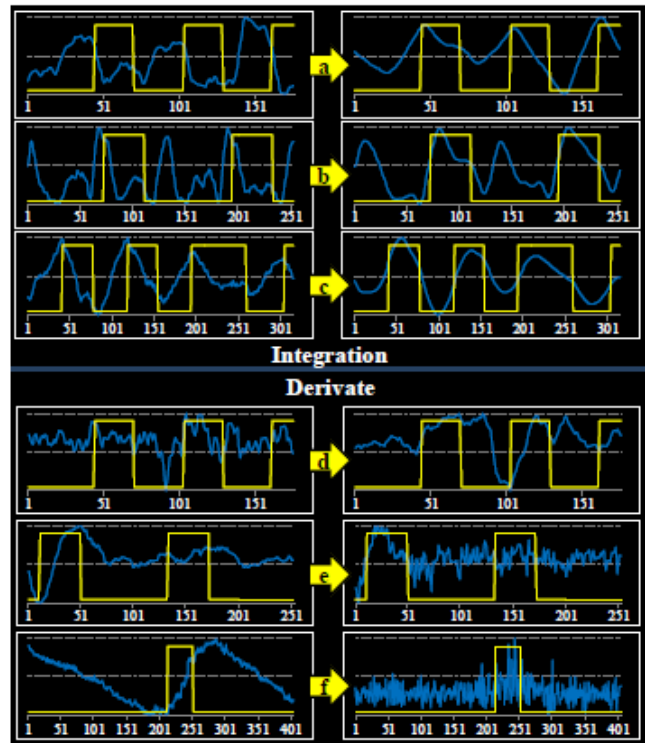


Fig.2. Time series of common functional components (blue) before (left) and after (right) applying the functional operators. Their corresponding contrast curve is plotted as yellow for reference. (a): Integration of component from emotion dataset; (b): Integration of component from gambling dataset; (c): Integration of component from language dataset; (d): Derivative of component from emotion dataset; (e): Derivative of component from gambling dataset; (f): Derivative of component from WM dataset.

3. RESULTS

3.1 Modulated functional components identified from HCP Q1 dataset

By applying the proposed framework on fMRI datasets of the seven tasks in HCP Q1 release, we have obtained the first and second level sparse representation of fMRI data. By using the Pearson correlation to identify functional components in the second stage, we compared all the modulated time series with the task stimulus and found that there are strong correlations between the integral-modulated components and stimulus (average correlation value: 0.71 ± 0.04 , $p < 0.05$), as well as relatively weaker correlation of the derivate-modulated components (average correlation value: 0.25 ± 0.05 , $p < 0.05$). One example is shown in Fig. 2, illustrating the identified task-evoked functional component modulation and their original temporal activation pattern from three different tasks. The improvement by applying the operator on the functional components shows the possible existence of brain networks responding to the external stimulus through modulation.

3.2 Refinement of activation detection result by functional operators

By using the trace-back method in Section 2.5, we have obtained the individual-level functional components corresponding to the group-level results which are likely to be modulated according to the analysis in Section 3.1. One illustration of the individual-level results is shown in Fig 3. From the relationships between spatial distributions of GLM-based activation detection results and the functional operator analysis results, we argue that the activation detection result is actually an aggregation of functional networks at various modulation levels. In other words, the response of the functional brain to the external stimulus could be non-linear and represented in the state space, where the traditional linear activation detection could not differentiate such modulations. For example, the spatial overlap ratio between the activation detection result and components identified by integral operator is 60.85%, and the spatial overlap between activation detection result and derivative operator is 51.87%, where integral and derivative-modulated component would have different spatial maps. Parts of the parietal cortex are activated in integral-modulated component, but rarely activated in derivative-modulated components. However, near angular areas and parts of the frontal cortex (pars triangularis and middle frontal area) are more involved in derivative-modulated components compared with integral-modulated components. As further shown in Fig. 3(c), the original temporal pattern of the components from functional operator results do not necessarily follow task design, thus there also exist regions that are not presented in the activation detection result but in the operator-modulated components.

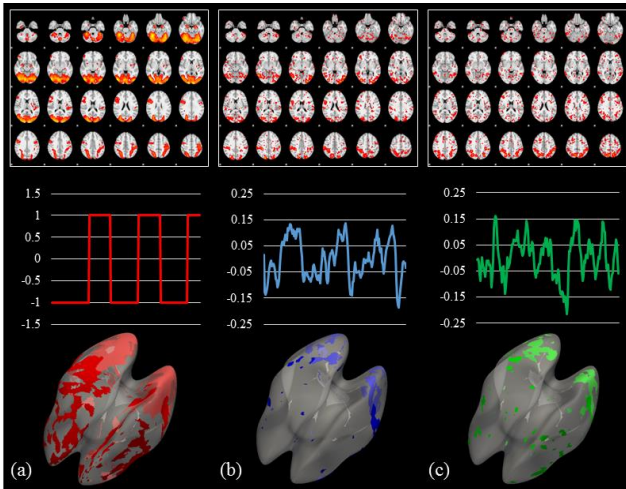


Fig.3. Example of the emotion task. (a) Activation detection result by GLM. (b) Functional component by integral operator analysis. (c) Functional component by derivative operator analysis.

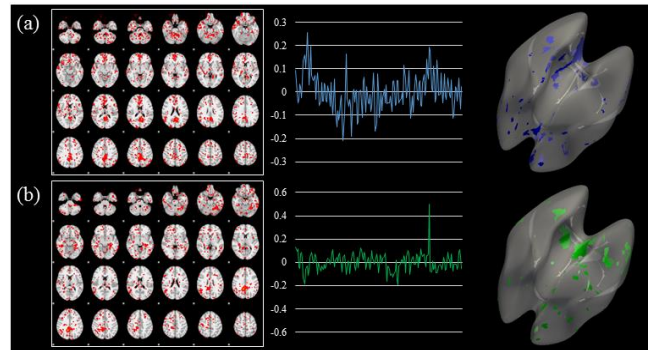


Fig.4. Example of the supplementary areas supported by operators. (a) Integral operator (b) Derivative operator

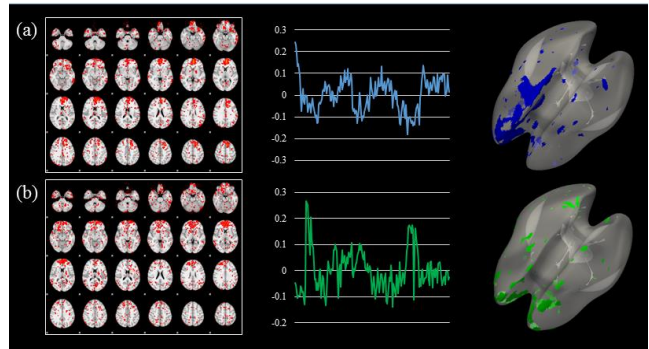


Fig.5. Another example of the supplement areas supported by operators. (a) Integral operator (b) Derivative operator

For example, the temporal pattern of the two operator-modulated components in Fig.4 have strong correlation with external stimulus (after modulation), but their spatial patterns are not included in the GLM activation results. Though the temporal patterns of operator-modulated components in Fig.5 are quite different, both of them could be identified by the proposed framework.

4. DISCUSSION AND CONCLUSION

In this work, we have introduced the concept of “functional operator”, aiming to provide a refinement and supplement to the GLM-based activation detection methods. The current concept and the corresponding framework contain two operators, the integral and derivative, which could provide three diversifications for the traditional GLM-based activation detection results and could be helpful in refining the detailed activation areas. We envision that the operator-based modelling could provide a new perspective in functional brain analysis, as the relationship across regions could be represented in the functional state-space based on their corresponding operators.

5. REFERENCES

- [1] Worsley, K. J. An overview and some new developments in the statistical analysis of PET and fMRI data. *Human Brain Mapping*, 5(4), 254-258, 1997.

- [2] Beckmann, C. F., Jenkinson, M., & Smith, S. M. General multilevel linear modeling for group analysis in FMRI. *Neuroimage*, 20(2), 1052-1063, 2003.
- [3] Friston, K. J., Holmes, A. P., Worsley, K. J., Poline, J. P., Frith, C. D., & Frackowiak, R. S. Statistical parametric maps in functional imaging: a general linear approach. *Human brain mapping*, 2(4), 189-210, 1994.
- [4] Van Den Heuvel, M. P., & Pol, H. E. H. Exploring the brain network: a review on resting-state fMRI functional connectivity. *European Neuropsychopharmacology*, 20(8), 519-534, 2010.
- [5] Bennett, S. A brief history of automatic control. *IEEE Control Systems Magazine*, 16(3), 17-25, 1996.
- [6] Chee F, Fernando T L, Savkin A V, et al. Expert PID control system for blood glucose control in critically ill patients[J]. *Information Technology in Biomedicine, IEEE Transactions on*, 7(4): 419-425, 2003.
- [7] Mairal, J., Bach, F., Ponce, J., & Sapiro, G. Online dictionary learning for sparse coding. In *Proceedings of the 26th Annual International Conference on Machine Learning* (pp. 689-696). ACM, 2009.
- [8] Kreutz-Delgado, K., Murray, J. F., Rao, B. D., Engan, K., Lee, T. W., & Sejnowski, T. J. Dictionary learning algorithms for sparse representation. *Neural computation*, 15(2), 349-396, 2003.
- [9] Lv, J., Jiang, X., Li, X., Zhu, D., Chen, H., Zhang, T., ... & Liu, T. Sparse representation of whole-brain FMRI signals for identification of functional networks. *Medical image analysis*, 20(1), 112-134, 2015.
- [10] Lv, J., Jiang, X., Li, X., Zhu, D., Zhang, S., Zhao, S., ... & Liu, T. Holistic Atlases of Functional Networks and Interactions Reveal Reciprocal Organizational Architecture of Cortical Function. *Biomedical Engineering, IEEE Transactions on*, 62(4), 1120-1131, 2015.
- [11] Zhang, S., Li, X., Lv, J., Jiang, X., Guo, L., & Liu, T. Characterizing and differentiating task-based and resting state fMRI signals via two-stage sparse representations. *Brain imaging and behavior*, 1-12, 2015.
- [12] Brett, M., Johnsrude, I. S., & Owen, A. M. The problem of functional localization in the human brain. *Nature reviews neuroscience*, 3(3), 243-249, 2002.
- [13] Stöcker, T., Schneider, F., Klein, M., Habel, U., Kellermann, T., Zilles, K., & Shah, N. J. Automated quality assurance routines for fMRI data applied to a multicenter study. *Human brain mapping*, 25(2), 237-246, 2005.
- [14] Barch, D. M., Burgess, G. C., Harms, M. P., Petersen, S. E., Schlaggar, B. L., Corbetta, M., ... & WU-Minn HCP Consortium. Function in the human connectome: task-fMRI and individual differences in behavior. *Neuroimage*, 80, 169-189, 2013.
- [15] Li, Y., Long, J., He, L., Lu, H., Gu, Z., & Sun, P. A sparse representation-based algorithm for pattern localization in brain imaging data analysis, 2012.